Analysis and Elimination of Grating Disk Inclination Error in Photoelectric Displacement Measurement

Hai Yu, Qiuhua Wan, Lihui Liang, and Changhai Zhao

***Abstract*—As core elements of photoelectric displacement measurement, installation coaxiality and rotation parallelism are the main factors affecting measurement accuracy. When there is a processing error or an offset in the installation process of structural elements, the plane of the grating disk will be tilted, which seriously affects the accuracy of angular displacement measurements. In this study, error caused by inclination of the grating disk was analyzed and a method to eliminate this error presented. First, an error model was established by analyzing the mechanism of measurement error caused by grating disk tilting, analysis showed that the error caused by grating disk tilt showed a "double cycle" fluctuation in the circle. Then, by using "double cycle" fluctuation, a method for eliminating errors was presented. Finally, the validity of the proposed theory and method was verified by simulation and experimentation. To eliminate errors, angular displacement measurements needed to be made using at least three reading heads to produce a mean. In these experiments, when the grating disk was tilted, the error was perfectly eliminated using three reading head measurements. The experimental results verified the validity of the proposed theory, which provided a theoretical basis for improving the displacement measurement accuracy.**

***Index Terms*—Error analysis, grating disk tilt, optical displacement measurement, three reading heads.**

I. Introduction

DIGITAL displacement measurement technology is the core displacement feedback component in industrial equipment [1], [2]. In photoelectric displacement measurement technology, the circular grating is used as the calibration element and marked lines on the circular grating identified through a photoelectric conversion module, so as to achieve digital output of the angular displacement through signal processing [3], [4]. Photoelectric displacement measurement technology has been widely used because of its strong anti-interference and easy to achieve large range measurement. With the development of high-performance numerical control machines, precision servo control, and other fields, photoelectric displacement measurement technology has been developing toward higher measurement accuracy. It has become the demand of current industrial applications to realize a method that is simple and easy to install and can ensure measurement accuracy [5], [6].

At present, improving the precision of photoelectric displacement measurements has become a research hotspot. In some studies, improving the interpolation accuracy of photoelectric measurement signals is an important method for improving measurement accuracy. For example, in 2018, Ye et al. [7] proposed a high-precision interpolation algorithm for sinusoidal signals to reduce the interpolation error to ± 0.0108 μm within the period of sinusoidal signals. In 2020, Chen et al. [8] proposed a self-adaptive interpolation method, with maximum interpolation number of 400, and actual measured interpolation errors within -1.2 to 1.1". At the same time, the self-calibration of long period error can be achieved by placing multiple reading heads in the circumference. For example, in 2001, Watanabe et al. [9] analyzed an error model generated by different axes of the grating disk and used multiple reading heads to correct the error. In 2008, Probst [10] proposed a method for self-calibration of divided circles, which is based on a known prime factor algorithm for the discrete Fourier transform to realize self-calibration of measurement errors. In 2013, Su et al. [11] used four reading heads to improve the measurement accuracy. In addition, error compensation for displacement measurement results is also an important means for improving measurement accuracy. For example, in 2005, Tan [12] proposed a method to calibrate the measured signal online using radial basis function. In 2007, Lu [13] proposed the automatic correction time measurement dynamic reversal method for angular displacement measurement. In 2017, Cai et al. [14] proposed a method based on empirical mode decomposition, which extracts the potential trend of measurement error and improves the measurement accuracy.

In our previous research, studies have focused on high-precision angular displacement measurement technology with double reading heads for convenient installation [15]. In following research, using an odd number of reading heads was

Manuscript received 8 April 2023; revised 3 June 2023; accepted 4 July 2023. This work was supported in part by the Natural Science Foundation of Jilin Province under Grant 20230101111JC, in part by National Natural Science Foundation of China under Grant 52075520, in part by Jilin Scientific and Technological Development Program under Grant 20210201097GX, and in part by Youth Innovation Promotion Association of the Chinese Academy of Sciences under Grant 2022221. *(Corresponding author: Hai Yu.)*

The authors are with the Changchun Institute of Optics, Fine Mechanics and Physics, Chinese Academy of Sciences, Changchun 130033, China (e-mail: yuhai@ciomp.ac.cn; wanqh@ciomp.ac.cn; lianglihui@ciomp.ac.cn; zhaoch@ciomp.ac.cn).

Color versions of one or more figures in this article are available at https://doi.org/10.1109/TIE.2023.3294641.

Digital Object Identifier 10.1109/TIE.2023.3294641

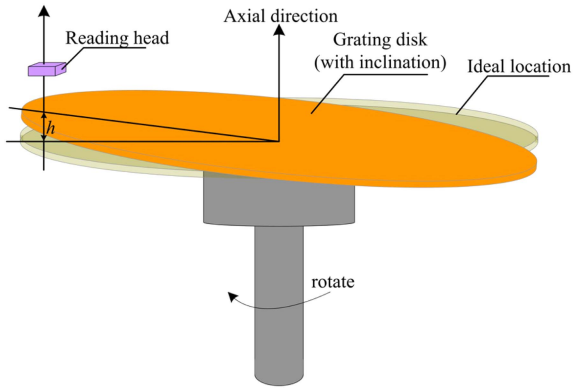

Fig. 1. Nonparallel schematic diagram.

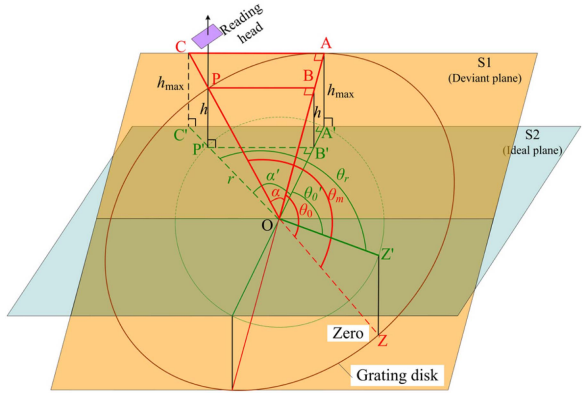

Fig. 2. Schematic diagram of grating disk tilt.

found to be easier for achieving high-precision measurement than an even number of reading heads [16]. In addition, work has been performed on improving the accuracy of angular displacement measurement using multiline fusion [17]. In previous research, when the grating disk is installed with inclination, it was found that the error generated cannot be ignored. But, at present, the mechanism of grating disk tilt error is still undefined and the principle for eliminating grating disk tilt error remains unclear. For this reason, in this study, the error caused by the tilt of the grating disk installation was examined. First, an error model was created when the grating disk was tilted. Then, a method was proposed to eliminate errors through model analysis. Finally, the correctness of our conclusions was verified by simulation and experimentation.

The structure of this article is as follows: Section II described the error model generated when the grating disk was installed obliquely, Section III provided methods for eliminating errors, simulation is given in Section IV, and Section V gives experimental verification. Finally, Section VI concludes the article.

II. Inclination Error Model

A. Error Model Derivation

In grating displacement measurement, as the calibration element of angular displacement measurement, the accuracy of the calibration grating installation will directly affect the accuracy of angular displacement measurement. When the installation plane of the grating disk is "inclined," the grating plane will not be parallel to the rotation plane of the rotation axis (see Fig. 1).

The grating disk rotates with the spindle and the reading head is relatively fixed (see Fig. 1). When the grating disk rotates, the vertical deviation h of the grating disk at the reading head position occurs. With rotation of the grating disk, the size of h will also change.

To facilitate analysis, the center of the circular grating was assumed not to deviate from the center of spindle rotation; that is, there is no eccentric error. In an ideal state, the plane where the grating disk is located is $S2$. When there is inclination, the plane of grating disk becomes $S1$ (see Fig. 2). At this time, the mapping position of the reading head on $S2$ plane is P'. The mapping point in $S1$ plane is P. When the grating disk rotates, the mapping points of the reading head on $S2$ plane fall within the circumference of radius r. When the reading head is at A', the vertical offset generated by the tilt of the grating disk reaches the maximum value $h = h_{\max}$.

The included angle between the reading head position P and point A on the $S1$ plane was $\angle \mathrm{POA} = \alpha$ (see Fig. 2). The included angle between P' and A' on $S2$ plane was $\angle \mathrm{P'OA'} = \alpha'$. At the same time, $\mathrm{P'O} = \mathrm{A'O} = r$. In $\triangle \mathrm{AOA'}$, there were $\mathrm{A'O} = r$ and $\mathrm{B'O} = r{\cdot}\cos\alpha'$. Therefore, the vertical offset at the mapping position P of the reading head is shown in (1), expressed as

$$h = PP' = BB' = \frac{B'O}{A'O} h_{\max} = h_{\max} \cos\alpha'. \tag{1}$$

At the same time, in $\triangle AOC$ of $S1$ plane, it was deduced that

$$AO = \sqrt{h_{\max}^2 + r^2} \text{ and}$$

$$CO = AO/\cos\alpha = \frac{\sqrt{h_{\max}^2 + r^2}}{\cos\alpha}.$$

In $\triangle COC'$, it was deduced that

$$C'O = \sqrt{CO^2 - h_{\max}^2} = \sqrt{\frac{h_{\max}^2 \cdot \sin^2\alpha + r^2}{\cos^2\alpha}}$$

$$h = h_{\max} \frac{P'O}{C'O} = \frac{r \cdot \cos\alpha \cdot h_{\max}}{\sqrt{r^2 + h_{\max}^2 \cdot \sin^2\alpha}}. \tag{2}$$

According to (1), it was deduced that the actual included angle between the reading head mapping position P′ and point A′ was

$$\alpha' = \angle P'OA' = \arccos\left(\frac{h}{h_{\max}}\right). \tag{3}$$

Entering (2) into (3) and simplifying obtained the included angle α' on $S2$ plane between the reading head position mapping point P′ and point A′, thus producing (4), expressed as

$$\alpha' = f(\alpha) = \arccos\left[\frac{r \cdot \cos\alpha}{\sqrt{r^2 + h_{\max}^2 \cdot \sin^2\alpha}}\right] \tag{4}$$

where $f(\alpha)$ represents the angle function mapped to $S2$ plane when the angle between $S1$ plane and AO line is α.

The zero point position read from the grating disk was set at Z and the included angle between the zero point

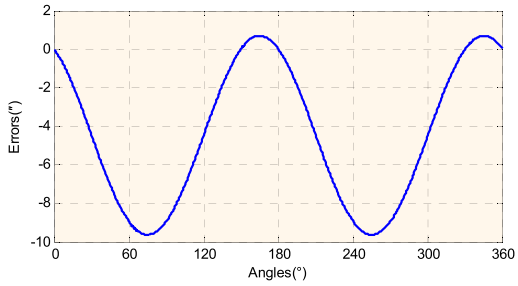

Fig. 3. Error simulation curve.

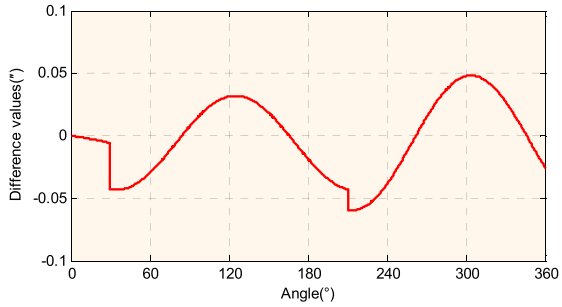

Fig. 4. Deviation of approximate expression of error.

position and point A position in $S1$ plane at $\angle ZOA = \theta_0$ (see Fig. 2). When the angle value read by the reading head was $\angle ZOC = \theta_m$, the included angle between the reading head point P and point A on the $S1$ plane became $\angle POA = \alpha = \theta_m\text{-}\theta_0$. Then, the actual angle value corresponding to θ_m was $\theta_r = \theta'_0 + \alpha' = f(\theta_0) + f(\theta_m - \theta_0)$. After (4) was brought in, it was expressed as

$$\theta_r = f(\theta_0) + f(\theta_m - \theta_0) = \arccos\left[\frac{r \cdot \cos\theta_0}{\sqrt{r^2 + h_{\max}^2 \cdot \sin^2\theta_0}}\right] + \arccos\left[\frac{r \cdot \cos(\theta_m - \theta_0)}{\sqrt{r^2 + h_{\max}^2 \cdot \sin^2(\theta_m - \theta_0)}}\right]. \quad (5)$$

Therefore, when the displacement data read by the reading head was θ_m, the angular displacement measurement error generated was (6), expressed as

$$\begin{aligned}\mu &= \theta_m - \theta_r \\ &= \theta_m - \arccos\left[\frac{r \cdot \cos\theta_0}{\sqrt{r^2 + h_{\max}^2 \cdot \sin^2\theta_0}}\right] \\ &\quad - \arccos\left[\frac{r \cdot \cos(\theta_m - \theta_0)}{\sqrt{r^2 + h_{\max}^2 \cdot \sin^2(\theta_m - \theta_0)}}\right]. \quad (6)\end{aligned}$$

B. Approximate Expression of Error Model

In order to facilitate subsequent analysis, we need to simplify or approximate the error model in (6).

According to (6), when the angle value θ_m obtained by the reading head changed from 0 to 360°, assume $\theta_0 = \pi/6$ and the radian error in (6) was converted into angle error $\mu\cdot(180^\circ/\pi)$ for simulation. We set $h_{\max} = 0.5$, r = 50 mm, the error curve of $\mu(h_{\max} = 0.5)$ is shown in Fig. 3.

By observing the error curve in Fig. 3, it can be observed that the error curve was seen to approximately possess a "double period" sine curve within the circle.

For convenience of analysis, the error model in (6) was approximately expressed as a "double periodic sine function." Then, the error caused by the tilt of the grating disk was approximate to

$$\mu \approx -U\sin[2(\theta_m - \theta_0)] + V \quad (7)$$

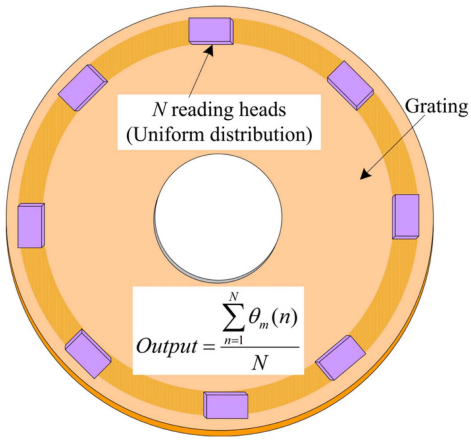

Fig. 5. Distribution of N reading heads.

where U represents the amplitude of error change, and V represents the dc component. Based on the error values in Fig. 3, we used (7) for fitting to determine the parameters U and V. Finally, we determined the coefficients as $U = -5.15$ and $V = -4.46$. Therefore, the error model is approximated as: $\mu'(h_{\max} = 0.5) = 4.46 \bullet \sin[2(\theta_m - \theta_0)] + 5.16$.

Meanwhile, to observe the difference between μ and μ', we have drawn the difference curve of μ-μ' in Fig. 4.

It can be seen that the difference between the error model and the approximate expression is in the range of ±0.06", which is very small. Therefore, we can approximate the error model as a double period sine curve (7).

III. Inclination Error Elimination

In order to eliminate the error value caused by tilt of the grating disk, multiple reading heads were used, installed in the circumference of the circular grating and the average of their measurements used as the final measurement result.

Assuming that the circumference contained N reading heads and the difference angle between N reading heads was assumed to be $360^\circ/N$ (see Fig. 3).

The θ_m is the measured value of the first reading head (see Fig. 5). Then, on the grating disk plane $S1$, the angle value read by the nth reading head is θ_m+(n-1)·$2\pi/N$ ($n = 1, 2, \ldots, N$). We use the approximate error model equation in Fig. 7 to calculate the error. After averaging N reading heads, the resultant error

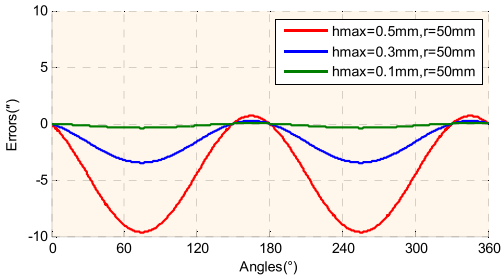

Fig. 6. Error simulation curve of different inclinations.

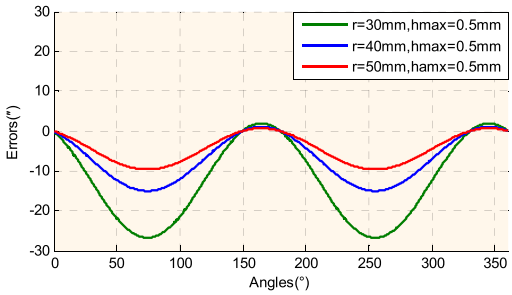

Fig. 7. Error curve of different radius.

was obtained from (8), expressed as

$$\mu\,|_N = \frac{\sum_{n=1}^{N}\{-U\sin[2\theta_m - 2\theta_0 + 2\pi(n-1)/N]\}}{N} + V. \tag{8}$$

To calculate the measurement error using different numbers of reading heads, respectively, set N was set to 2, 3, and 4. The resulting related errors were

$$\begin{aligned}\mu|_{N=2} =& -U\{\sin[2(\theta_m-\theta_0)]\\ &+\sin[2(\theta_m-\theta_0+\pi)]\}/2+V\\ =& -U\sin[2(\theta_m-\theta_0)]+V \end{aligned}\tag{9}$$

$$\begin{aligned}\mu|_{N=3} =& -U\{\sin[2(\theta_m-\theta_0)]\\ &+\sin[2(\theta_m-\theta_0+2\pi/3)]\\ &+\sin[2(\theta_m-\theta_0+4\pi/3)]\}/3+V\\ =& -U\{\sin[2(\theta_m-\theta_0)]\\ &-\sin[2(\theta_m-\theta_0)]\cos(\pi/3)\\ &-\cos[2(\theta_m-\theta_0)]\sin(\pi/3)\\ &+\sin[2(\theta_m-\theta_0)]\cos(2\pi/3)\\ &+\cos[2(\theta_m-\theta_0)]\sin(2\pi/3)\}/3+V\text{and}\\ =& V \end{aligned}\tag{10}$$

$$\begin{aligned}\mu|_{N=4} =& -U\{\sin[2(\theta_m-\theta_0)]\\ &+\sin[2(\theta_m-\theta_0+\pi/2)]\\ &+\sin[2(\theta_m-\theta_0+\pi)]\\ &+\sin[2(\theta_m-\theta_0+3\pi/2)]\}/4+V\\ =& -U\{\sin[2(\theta_m-\theta_0)]+\cos[2(\theta_m-\theta_0)]\\ &-\sin[2(\theta_m-\theta_0)]-\cos[2(\theta_m-\theta_0)]\}/4+V\\ =& V. \end{aligned}\tag{11}$$

It can be seen that when $N = 2$, the combined measurement error of double reading heads $\mu|_{N=2}$ was not eliminated. When $N > 2$, the combined error of multiple reading heads became $\mu|_{N=3} = V$ and $\mu|_{N=4} = V$. As V was a dc component, error could be eliminated when $N > 2$. According to the above, it was concluded that, in the angular displacement measurement of the circular grating, to eliminate error caused by grating disk tilt, at least three reading heads should be uniformly distributed around the circumference to achieve error correction.

IV. Simulation

To verify the conclusions obtained from the above analysis and simulate the error curve, the radius of the grating disk was set at 50 mm, maximum vertical offset $h_{\max}$ due to tilt of the grating disk at 0.5 mm, and difference angle θ_0 between the zero position and maximum vertical offset position of the grating disk as $30^\circ\times(\pi/180^\circ) = \pi/6$.

A. Error Simulation of Tilt Change

According to (6), when the angle value θ_m obtained by the reading head changed from 0° to 360°, the radian error in (6) was converted into angle error $\mu\cdot(180^\circ/\pi)$ for simulation. During simulation, to observe the change degree of the error curve, the maximum vertical offsets were respectively set to $h_{\max} = 0.5$, 0.3, and 0.1 mm (see Fig. 6).

It was seen that, when $h_{\max}$ gradually increased, the error amplitude also gradually increased. When $h_{\max} = 0.5$ mm, the error fluctuation amplitude was about $U \approx 5''$.

B. Error Simulation When Grating Radius Changes

Assuming that $h_{\max}$ of 0.5 mm remained unchanged, the errors when the radius of the grating disk were 30, 40, and 50 mm were simulated (see Fig. 7).

When the maximum offset of the grating disk was unchanged, the amplitude of the error fluctuation was observed to decrease with increased disk radius. When the radius was 30 mm, the error fluctuation amplitude was approximately $U \approx 15"$.

Therefore, it was concluded that, when the variation of vertical offset of the grating disk was constant, the larger the disk radius was, the smaller the error fluctuation amplitude (see Fig. 7).

C. Simulation of Multiple Readers

The error was then simulated when the circumference contained 2, 3, or 4 reading heads (see Fig. 8).

During simulation, the radius was set at 50 mm, maximum vertical offset due to nonparallel installation of the grating disk at $h_{\max} = 0.5$ mm, and difference angle between the zero position and maximum vertical offset position at $\theta_0 = 30^\circ\times(\pi/180^\circ)$.

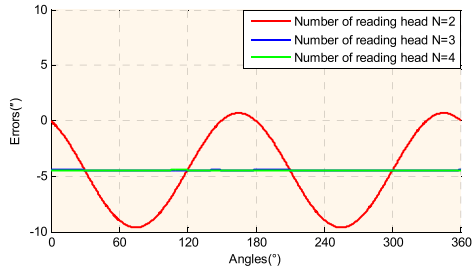

Fig. 8. Error curve of different quantity reading heads.

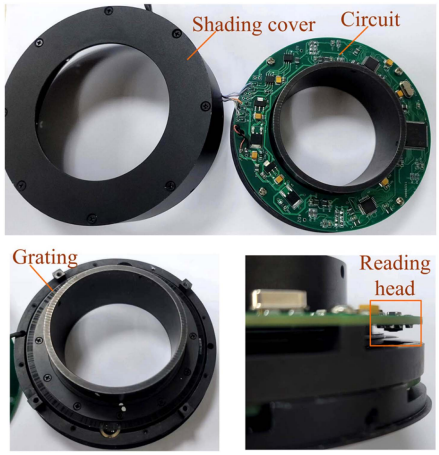

Fig. 9. Experimental devices.

The simulation curve when the number of reading heads was $N = 2$, the fluctuation amplitude of the error curve was the same as the error curve when was $N = 1$. This showed that error caused by the tilt of the grating disk could not be eliminated by the uniform distribution of double reading heads within the circle of the grating disk.

At the same time, it was seen that, when the number of reading heads was $N \geq 3$, error was well eliminated, which was consistent with the conclusion in Section II. Therefore, to eliminate error caused by nonparallelism between the grating encoder and the rotating plane, at least three reading heads should be used.

V. Experiments

A. Test of Experimental Device

To verify the proposed conclusions, angular displacement measuring device was designed for experiments using the image displacement measurement method [16], [17] proposed earlier (see Fig. 9). In the grating disk used, the center radius of the marked line is $r = 48$ mm, and there are 512 period lines within the circumference of the grating. The measurement device can achieve resolution better than 25 bit, and the output data noise fluctuation is less than $0.04''$. As the "image-type displacement measurement" adopted the full digital signal processing method, it was not affected by "deviation from the ideal state" of the measurement signal. Therefore, it was not necessary to consider error caused by the measurement signal offset in the experiment

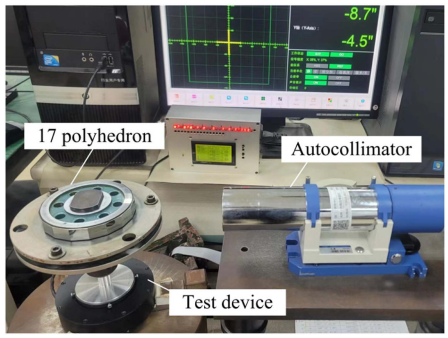

Fig. 10. Principle of error calibration.

TABLE I
Errors Without Inclination

Order No.	Errors, "	Order No.	Errors, "
1	0	10	−5.8
2	1.3	11	−2.2
3	0.3	12	−0.2
4	−0.5	13	−0.6
5	1.3	14	1.9
6	7.9	15	11.8
7	11.7	16	5.7
8	6.3	17	0.8
9	−1.3		

and thus easier to observe error results caused by grating disk tilt.

On the grating disk used here, the code path radius was 48 mm. During installation, the coaxiality between the grating disk and rotating spindle were carefully adjusted through a microscope ($\leq \pm 0.01$mm), so as to minimize the error impact caused by the eccentricity of the encoder.

According to the analysis in Section III, when $N = 2$, the measurement error amplitude obtained was the same as that with $N = 1$.

At the same time, according to our previous research [15], using a double reading head can eliminate error interference from different axes of the grating disk. Therefore, to accurately observe the error caused by the tilt of the encoder disk, a double reading head was used to obtain the error amplitude caused by grating disk tilt. During error tests, 17 polyhedrons were used to coaxially connect with the experimental device. Through calibration of the photoelectric autocollimator, 17 error-sampling points were obtained. The principle of error calibration is shown in Fig. 10.

The measurement error obtained using the 17-polyhedron test is shown in Table I. When the grating was not tilted, the error fluctuation amplitude was seen to be -5.8–$11.8''$, error fluctuation amplitude is $8.8''$, and mean square error 4.83".

B. Test When the Grating Disk is Tilted

To obtain the error caused by grating disk tilt, the grating disk of the experimental device was deliberately tilted to make it swing in the vertical direction when it rotated. The experimental device was fixed on the platform and a micrometer used to measure the vertical offset of the grating disk (see Fig. 11). During a measurement, a random position within the circle of

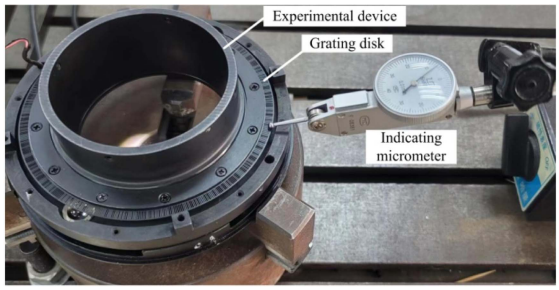

Fig. 11. Measurement of grating disk inclination.

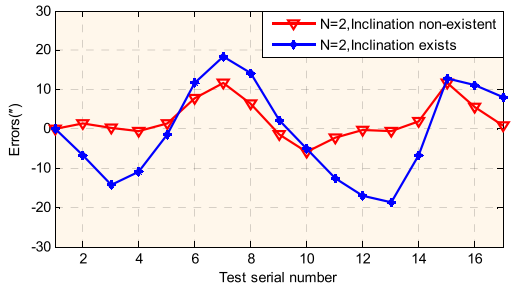

Fig. 12. Error comparison before and after grating disk is inclined.

TABLE II
VERTICAL OFFSET

Order No.	Vertical offset, mm	Order No.	Vertical offset. mm
1	0	7	−0.25
2	0.23	8	−0.29
3	0.37	9	−0.37
4	0.16	10	−0.43
5	−0.11	11	−0.23
6	−0.22	12	−0.17

TABLE III
ERROR IN CASE OF INCLINATION

Order No.	Errors, "	Order No.	Errors, "
1	0	10	−4.9
2	−6.8	11	−12.5
3	−14.4	12	−16.9
4	−10.8	13	−18.6
5	−1.3	14	−6.8
6	11.8	15	12.7
7	18.5	16	11.1
8	14.1	17	8.2
9	2.1		

the grating disk was selected as the measurement starting point and a total of 12 points measured. The vertical offset obtained by the test is shown in Table II.

It can be seen that the maximum value of vertical offset h within the circumference range was 0.37 mm, minimum value −0.43 mm, and variation amplitude (0.37+0.43)/2 = 0.4 mm. Therefore, the offset $h_{\max} = 0.4$ mm in (6).

To ensure consistency in the experiment, the coaxiality between the grating disk and rotating spindle were also carefully adjusted through a microscope ($\leq \pm 0.01$ mm). When the grating was offset, the measurement error of the 17-polyhedron acquisition experimental device was determined (see Table III). The error fluctuation range became −18.6–18.5″, error fluctuation amplitude is 18.55″, and error standard deviation increased to 11.85" (see Table III).

The error curve before and after the grating was tilted showed that, when the grating disk was tilted, the fluctuation amplitude of the error curve became significantly larger and the error curve showed a "double period" fluctuation in the circumference (Fig. 12).

Through comparison, it can be seen that the error amplitude increased by 18.55″-8.8″ = 9.75" before and after the code disk was tilted. This was consistent with the error model in (7).

TABLE IV
ERROR OF THREE READING HEADS

Order No.	Errors, "	Order No.	Errors, "
1	0	10	−8.8
2	−8.3	11	−2.9
3	−2.5	12	−6.1
4	−7.6	13	−3.1
5	−4.2	14	−8.1
6	−3	15	−1.7
7	−2.6	16	−9.1
8	−4.2	17	−4.8
9	−7.6		

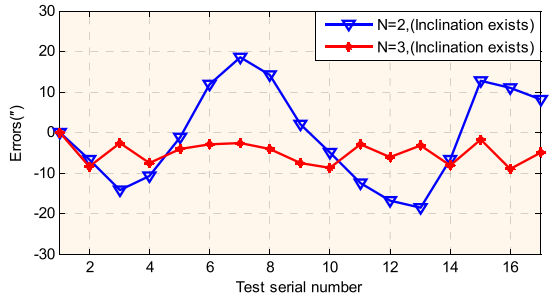

Fig. 13. Error comparison curve.

C. Error Elimination Experiment

To verify the effect of measuring with multiple reading heads and eliminating the tilt error of the grating disk, three reading heads were used to measure angular displacement. In experiments, three identical reading heads were uniformly installed in the circumference of the circular grating and the measurement results of the three reading heads taken to be the angular displacement measurement. When the measurement error of three reading heads was calibrated with the 17 polyhedrons, error values were obtained (see Table IV) and an error curve produced (see Fig. 13, red curve). For contrast, these measurement results were compared for $N = 2$ (blue curve).

When $N = 3$, error was obtained from angular displacement measurements, with the curve fluctuation range 0∼ −9.1″, error fluctuation amplitude 4.55″, and error standard deviation 2.83" (see Fig. 13). When three reading heads were used for measurement, the error fluctuation range was clearly smaller than when $N = 2$. Therefore, this demonstrated that the error from grating offset was clearly eliminated when using three reading heads.

VI. Conclusion

This study analyzed the principle of angular displacement measurement error when the grating disk was tilted and proposed a method for eliminating tilt error. First, an error model was established when the grating disk was tilted. Second, through analysis of the error model, measures for eliminating this error were determined. Third, the error model was simulated and analyzed. Finally, the proposed theory was verified by designing an experimental device. When the code path center radius of the grating disk was 48 mm, tests were performed and measurement errors compared before and after the grating disk was tilted. The results showed that when the grating disk was tilted (the vertical offset of the encoder disk changed by ± 0.4 mm), the measurement error was significantly eliminated by three reading heads (the mean square deviation of error reduced to 2.83").

Through simulation and experimental analysis, the following conclusions were obtained:

1) When the grating disk was inclined, the angular displacement measurement error curve generated showed a "double cycle" fluctuation in the circumference.
2) When the center radius of the code path on the grating disk was constant, the larger the tilt of the grating disk was, the greater the error fluctuation amplitude. At the same time, when the vertical offset amplitude caused by the grating tilt was constant, the larger the grating disk radius was, the smaller the error.
3) When N reading heads were used to take the mean value for error correction, double reading heads could not eliminate the error caused by grating disk tilt.
4) To eliminate error caused by grating disk tilt, $N \geq 3$ reading heads should be used and the mean value taken to achieve angular displacement measurements.

In conclusion, in addition to eccentric error, error caused by grating disk tilt cannot be ignored during the installation process. After analyzing the error model of the encoder tilt error, this study presented a method for eliminating this error. This research will provide a theoretical basis for the use of convenient installation in industrial applications to achieve high-precision measurements.

References

[1] Z. Yu, K. Peng, X. Liu, Z. Chen, and Y. Huang, "A high-precision absolute angular-displacement capacitive sensor using three-stage time-grating in conjunction with a remodulation scheme," *IEEE Trans. Ind. Electron.*, vol. 66, no. 9, pp. 7376–7385, Sep. 2019.

[2] N. Anandan and B. George, "A wide-range capacitive sensor for linear and angular displacement measurement," *IEEE Trans. Ind. Electron.*, vol. 64, no. 7, pp. 5728–5737, Jul. 2017.

[3] F. Liu et al., "Error analyses and calibration methods with accelerometers for optical angle encoders in rotational inertial navigation systems," *Appl. Opt.*, vol. 52, pp. 7724–7731, 2013.

[4] C. Yang and S. O. Oyadiji, "Theoretical and experimental study of self-reference intensity-modulated plastic fibre optic linear array displacement sensor," *Sensors Actuators: A. Phys.*, vol. 222, pp. 67–79, 2015.

[5] T. Dziwinski, "A novel approach of an absolute encoder coding pattern," *IEEE Sensors J.*, vol. 15, no. 1, pp. 397–401, Jan. 2015.

[6] H. Li et al., "Two-dimensional gold matrix method for encoding two-dimensional optical arbitrary positions," *Opt. Exp.*, vol. 26, pp. 12742–12754, 2018.

[7] G. Ye et al., "Ratiometric-linearization-based high-precision electronic interpolator for sinusoidal optical encoders," *IEEE Trans. Ind. Electron.*, vol. 65, no. 10, pp. 8224–8231, Oct. 2018.

[8] Z. Chen, X. Liu, K. Peng, Z. Yu, and H. Pu, "A self-adaptive interpolation method for sinusoidal sensors," *IEEE Trans. Instrum. Meas.*, vol. 69, no. 10, pp. 7675–7682, Oct. 2020.

[9] T. Watanabe et al., "Automatic high precision calibration system for rotary encoder," *J. Jpn. Soc. Precis. Eng.*, vol. 67, no. 7, pp. 1091–1095, 2001.

[10] R. Probst, "Self-calibration of divided circles on the basis of a prime factor algorithm," *Meas. Sci. Technol.*, vol. 19, no. 1, 2008, Art. no. 015101.

[11] D. Su, Z. Xv, J. Jia, B. Liu, and D. Li, "Read-head design for improving the precision of circular grating angular measuring system," *J. Electron. Meas. Instrum.*, vol. 27, pp. 653–657, 2013.

[12] K. K. Tan and K. Z. Tang, "Adaptive online correction and interpolation of quadrature encoder signals using radial basis functions," *IEEE Trans. Control Syst. Technol.*, vol. 13, no. 3, pp. 370–377, May 2005.

[13] X. D. Lu and D. L. Trumper, "Self-calibration of on-axis rotary encoders," *CIRP Ann.*, vol. 56, no. 1, pp. 499–504, 2007.

[14] N. Cai et al., "A novel error compensation method for an absolute optical encoder based on empirical mode decomposition," *Mech. Syst. Signal Process.*, vol. 88, pp. 81–88, 2017.

[15] H. Yu, Q. Wan, Y. Sun, X. Lu, and C. Zhao, "High precision angular measurement via dual imaging detectors," *IEEE Sensors J.*, vol. 19, no. 17, pp. 7308–7312, Sep. 2019.

[16] H. Yu, Q. Wan, X. Lu, C. Zhao, and L. Liang, "High precision angular displacement measurement based on self-correcting error compensation of three image sensors," *Appl. Opt.*, vol. 61, no. 1, pp. 287–293, 2022.

[17] H. Yu, Q. Wan, X. Lu, Y. Du, and L. Liang, "High precision displacement measurement algorithm based on depth fusion of grating projection pattern," *Appl. Opt.*, vol. 61, no. 4, pp. 1049–1056, 2022.

Hai Yu was born in Jilin province, China, in 1987. He received the B.S. degree in electronic information science and technology from Northeast Dianli University, Jilin, China, in 2009. He received the Ph.D. degree in mechanical and electronic engineering from University of Chinese Academy of Sciences, Beijing, China, in 2014.

Since 2017, he has been a Project Leader for several Natural Science Foundation of China and other agency-funded projects. He was funded by the "Dawn" talent training program of Changchun Institute of Optics, Fine Mechanics and Physics, Chinese Academy of Sciences (CIOMP), in 2020. He is currently an Associate Researcher with the R&D Center for Precision Instruments and Equipment, CIOMP. His research interest include electro-optical displacement precision measurement.

Dr. Yu became a member of the Youth Innovation Promotion Association of the Chinese Academy of Sciences, in 2022.

Qiuhua Wan was born in Jilin Province, China, in 1962. She received the Ph.D. degree in optical engineering from University of Chinese Academy of Sciences, Beijing, China, in 2009.

She is currently a Researcher with the R&D Center for Precision Instruments and Equipment, CIOMP. Her research interest include electro-optical displacement precision measurement.

Lihui Liang was born in Jilin province, China, in 1980. He received the Ph.D. degree in mechanical and electronic engineering from the University of Chinese Academy of Sciences, Beijing, China, in 2010.

He is currently an Associate Researcher with the R&D Center for Precision Instruments and Equipment, CIOMP. His research interest include electro-optical displacement precision measurement.

Changhai Zhao was born in Henan province, China, in 1980. He received the Ph.D. degree in mechanical and electronic engineering from University of Chinese Academy of Sciences, Beijing, China, in 2008.

He is currently an Associate Researcher with the R&D Center for Precision Instruments and Equipment, CIOMP. His research interest include electro-optical displacement precision measurement.